

Plasmon-induced transparency in twisted Fano terahertz metamaterials

Yingfang Ma,¹ Zhongyang Li,¹ Yuanmu Yang,¹ Ran Huang,² Ranjan Singh,³ Shuang Zhang,⁴ Jianqiang Gu,¹ Zhen Tian,¹ Jianguang Han,^{1,5} and Weili Zhang^{2,*}

¹Center for Terahertz Waves and College of Precision Instrument and Optoelectronics Engineering, Tianjin University, and Key Laboratory of Opto-electronics Information Technology, Ministry of Education, Tianjin 300072, China

²School of Electrical and Computer Engineering, Oklahoma State University, Stillwater, Oklahoma 74078, USA

³Center for Integrated Nanotechnologies, Materials Physics and Applications Division, Los Alamos National Laboratory, Los Alamos, New Mexico 87545, USA

⁴School of Physics and Astronomy, University of Birmingham, Birmingham B15 2TT, UK

⁵jiaghan@tju.edu.cn

* weili.zhang@okstate.edu

Abstract: We investigate the effect of tweaking the quality (Q) factor of split ring resonators in a coupled state, giving rise to plasmonic induced transparency (PIT) which has two distinct, individually engineered resonance modes. The Q factor and the amplitude of each resonance are tuned by twisting them mutually in the unit cell consisting of a subradiant and a superradiant resonator. We experimentally observe that introducing a gradual twist in the three U-shape resonators has a dramatic impact on the PIT spectral response, leading to the disappearance of the transparency peak beyond a certain critical degree of twist. This mainly happens due to the change in the in-plane coupling between the resonators as well the variation in coupling of the twisted resonators with the incident electric field. Further investigation based on the Fano model provides good agreement with the experimental results. The scheme presented here for controlling the Q factor of each resonator in the coupled regime is a unique way to tune the PIT response in terahertz metamaterials and can be easily scaled across the entire electromagnetic spectrum.

© 2011 Optical Society of America

OCIS codes: (160.3918) Metamaterials; (240.6680) Surface plasmons.

References and links

1. R. A. Shelby, D. R. Smith, and S. Schultz, "Experimental verification of a negative index of refraction," *Science* **292**(5514), 77–79 (2001).
2. D. Schurig, J. J. Mock, B. J. Justice, S. A. Cummer, J. B. Pendry, A. F. Starr, and D. R. Smith, "Metamaterial electromagnetic cloak at microwave frequencies," *Science* **314**(5801), 977–980 (2006).
3. J. B. Pendry, "Negative refraction makes a perfect lens," *Phys. Rev. Lett.* **85**(18), 3966–3969 (2000).
4. D. R. Smith, J. B. Pendry, and M. C. K. Wiltshire, "Metamaterials and negative refractive index," *Science* **305**(5685), 788–792 (2004).
5. J. Gu, J. Han, X. Lu, R. Singh, Z. Tian, Q. Xing, and W. Zhang, "A close-ring pair terahertz metamaterial resonating at normal incidence," *Opt. Express* **17**(22), 20307–20312 (2009).
6. R. Singh, C. Rockstuhl, C. Menzel, T. P. Meyrath, M. He, H. Giessen, F. Lederer, and W. Zhang, "Spiral-type terahertz antennas and the manifestation of the Mushlake principle," *Opt. Express* **17**(12), 9971–9980 (2009).
7. S. Zhang, D. A. Genov, Y. Wang, M. Liu, and X. Zhang, "Plasmon-induced transparency in metamaterials," *Phys. Rev. Lett.* **101**(4), 047401 (2008).
8. R. Singh, C. Rockstuhl, F. Lederer, and W. Zhang, "Coupling between a dark and a bright eigenmode in a terahertz metamaterial," *Phys. Rev. B* **79**(8), 085111 (2009).
9. P. Tassin, L. Zhang, T. Koschny, E. N. Economou, and C. M. Soukoulis, "Low-loss metamaterials based on classical electromagnetically induced transparency," *Phys. Rev. Lett.* **102**(5), 053901 (2009).
10. S.-Y. Chiam, R. Singh, C. Rockstuhl, F. Lederer, W. Zhang, and A. A. Bettiol, "Analogue of electromagnetically induced transparency in a terahertz metamaterial," *Phys. Rev. B* **80**(15), 153103 (2009).

11. C.-Y. Chen, I.-W. Un, N.-H. Tai, and T.-J. Yen, "Asymmetric coupling between subradiant and superradiant plasmonic resonances and its enhanced sensing performance," *Opt. Express* **17**(17), 15372–15380 (2009).
12. Y. Yang, R. Huang, L. Cong, Z. Zhu, J. Gu, Z. Tian, R. Singh, S. Zhang, J. Han, and W. Zhang, "Modulating the fundamental inductive-capacitive resonance in asymmetric double-split ring terahertz metamaterials," *Appl. Phys. Lett.* **98**(12), 121114 (2011).
13. N. Liu, L. Langguth, T. Weiss, J. Kästel, M. Fleischhauer, T. Pfau, and H. Giessen, "Plasmonic analogue of electromagnetically induced transparency at the Drude damping limit," *Nat. Mater.* **8**(9), 758–762 (2009).
14. R. D. Kekatpure, E. S. Barnard, W. Cai, and M. L. Brongersma, "Phase-coupled plasmon-induced transparency," *Phys. Rev. Lett.* **104**(24), 243902 (2010).
15. Y. Lu, J. Y. Rhee, W. H. Jang, and Y. P. Lee, "Active manipulation of plasmonic electromagnetically-induced transparency based on magnetic plasmon resonance," *Opt. Express* **18**(20), 20912–20917 (2010).
16. N. Papisimakis, V. A. Fedotov, N. I. Zheludev, and S. L. Prosvirnin, "Metamaterial analog of electromagnetically induced transparency," *Phys. Rev. Lett.* **101**(25), 253903 (2008).
17. R. Singh, E. Plum, C. Menzel, C. Rockstuhl, A. K. Azad, R. A. Cheville, F. Lederer, W. Zhang, and N. I. Zheludev, "Terahertz metamaterial with asymmetric transmission," *Phys. Rev. B* **80**(15), 153104 (2009).
18. A. Christ, O. J. Martin, Y. Ekinci, N. A. Gippius, and S. G. Tikhodeev, "Symmetry breaking in a plasmonic metamaterial at optical wavelength," *Nano Lett.* **8**(8), 2171–2175 (2008).
19. R. Singh, E. Plum, W. Zhang, and N. I. Zheludev, "Highly tunable optical activity in planar achiral terahertz metamaterials," *Opt. Express* **18**(13), 13425–13430 (2010).
20. V. A. Fedotov, M. Rose, S. L. Prosvirnin, N. Papisimakis, and N. I. Zheludev, "Sharp trapped-mode resonances in planar metamaterials with a broken structural symmetry," *Phys. Rev. Lett.* **99**(14), 147401 (2007).
21. R. Singh, I. A. I. Al-Naib, M. Koch, and W. Zhang, "Asymmetric planar terahertz metamaterials," *Opt. Express* **18**(12), 13044–13050 (2010).
22. J. Zhang, S. Xiao, C. Jeppesen, A. Kristensen, and N. A. Mortensen, "Electromagnetically induced transparency in metamaterials at near-infrared frequency," *Opt. Express* **18**(16), 17187–17192 (2010).
23. Q. Bai, C. Liu, J. Chen, C. Cheng, M. Kang, and H.-T. Wang, "Tunable slow light in semiconductor metamaterial in a broad terahertz regime," *J. Appl. Phys.* **107**(9), 093104 (2010).
24. V. Yannopoulos, E. Paspalakis, and N. V. Vitanov, "Electromagnetically induced transparency and slow light in an array of metallic nanoparticles," *Phys. Rev. B* **80**(3), 035104 (2009).
25. N. Papisimakis, Y. H. Fu, V. A. Fedotov, S. L. Prosvirnin, D. P. Tsai, and N. I. Zheludev, "Metamaterial with polarization and direction insensitive resonant transmission response mimicking electromagnetically induced transparency," *Appl. Phys. Lett.* **94**(21), 211902 (2009).
26. Z. Li, Y. Ma, R. Huang, R. Singh, J. Gu, Z. Tian, J. Han, and W. Zhang, "Manipulating the plasmon-induced transparency in terahertz metamaterials," *Opt. Express* **19**(9), 8912–8919 (2011).
27. J. Han, W. Zhang, W. Chen, L. Thamizhmani, A. K. Azad, and Z. Zhu, "Far-infrared characteristics of ZnS nanoparticles measured by terahertz time-domain spectroscopy," *J. Phys. Chem. B* **110**(5), 1989–1993 (2006).
28. R. Singh, A. K. Azad, J. F. O'Hara, A. J. Taylor, and W. Zhang, "Effect of metal permittivity on resonant properties of terahertz metamaterials," *Opt. Lett.* **33**(13), 1506–1508 (2008).
29. J. Gu, R. Singh, Z. Tian, W. Cao, Q. Xing, M. He, J. W. Zhang, J. Han, H.-T. Chen, and W. Zhang, "Terahertz superconductor metamaterial," *Appl. Phys. Lett.* **97**(7), 071102 (2010).
30. A. K. Azad, J. Dai, and W. Zhang, "Transmission properties of terahertz pulses through subwavelength double split-ring resonators," *Opt. Lett.* **31**(5), 634–636 (2006).
31. R. Singh, X. Lu, J. Gu, Z. Tian, and W. Zhang, "Random terahertz metamaterials," *J. Opt.* **12**(1), 015101 (2010).
32. E. Prodan, C. Radloff, N. J. Halas, and P. Nordlander, "A hybridization model for the plasmon response of complex nanostructures," *Science* **302**(5644), 419–422 (2003).
33. B. Luk'yanchuk, N. I. Zheludev, S. A. Maier, N. J. Halas, P. Nordlander, H. Giessen, and C. T. Chong, "The Fano resonance in plasmonic nanostructures and metamaterials," *Nat. Mater.* **9**(9), 707–715 (2010).
34. R. Singh, I. A. I. Al-Naib, M. Koch, and W. Zhang, "Sharp Fano resonances in THz metamaterials," *Opt. Express* **19**(7), 6312–6319 (2011).
35. A. E. Miroshnichenko, S. Flach, and Y. S. Kivshar, "Fano resonances in nanoscale structures," *Rev. Mod. Phys.* **82**(3), 2257–2298 (2010).
36. J. Han, A. K. Azad, M. Gong, X. Lu, and W. Zhang, "Coupling between surface plasmons and nonresonant transmission in subwavelength holes at terahertz frequencies," *Appl. Phys. Lett.* **91**(7), 071122 (2007).
37. R. Singh, C. Rockstuhl, F. Lederer, and W. Zhang, "The impact of nearest neighbor interaction on the resonances in terahertz metamaterials," *Appl. Phys. Lett.* **94**(2), 021116 (2009).
38. R. Singh, C. Rockstuhl, and W. Zhang, "Strong influence of packing density in terahertz metamaterials," *Appl. Phys. Lett.* **97**(24), 241108 (2010).

1. Introduction

Metamaterials offer enormous opportunities and unprecedented abilities to manipulate electromagnetic waves and have been extensively studied recently. The versatile character of metamaterials in many cases cannot be replicated by naturally occurring materials thus enabling promising applications such as negative refraction, invisibility cloaking,

superfocusing, and miniaturized antennas [1–6]. In pursuit of metamaterials with exotic electromagnetic behaviors, researchers have recently moved beyond the aforementioned implementations. A prime example is the mimicking quantum phenomena of electromagnetic induced transparency (EIT) or plasmon-induced transparency (PIT) phenomenon in classical metamaterial systems, which offers a smart route to exploit the unique outcome of coherent coupling in classical resonators. Efforts have recently been made with a series of micro- and nano-structures to realize the EIT-like effect, such as cut wires [6], split-ring-resonators (SRRs) [7–11], coupled waveguide micro-resonators and other multi-layer structures [12,13]. These works have theoretically and experimentally demonstrated that the EIT-like effect can be realized in metamaterials via destructive interference between different excitation pathways that are closely related to the symmetry breaking of the structures [6–26]. Seeking new designs to tune the EIT-like behavior for specific device needs are still in progress.

In general, to design a PIT metamaterial two resonance modes with an exactly identical resonance frequency but significantly different quality factors (Q -factor), namely a narrow high- Q mode and a broad low- Q mode, need to be excited simultaneously. The PIT spectral response is thus a result of coupling between the low- Q superradiant resonator and the high- Q subradiant resonator [7]. This is often viewed as an important strategy in the design of PIT metamaterials. As such, the PIT spectral response is sensitive to the variations in the sharpness of each resonance mode. If the Q factor of a particular resonator can be properly controlled by tailoring the metamaterial structure, we may tune the PIT spectral response, which is important for realizing photonic devices with enhanced functionalities. While previous works focused on the effect of coupling strength on PIT, here we show that the Q factor of the constituent elements in a “metamaterial molecule” plays a critical role in achieving the PIT spectral behavior. We experimentally and numerically demonstrate that when the Q factor of the constituent elements is altered via structure twisting, the PIT spectral

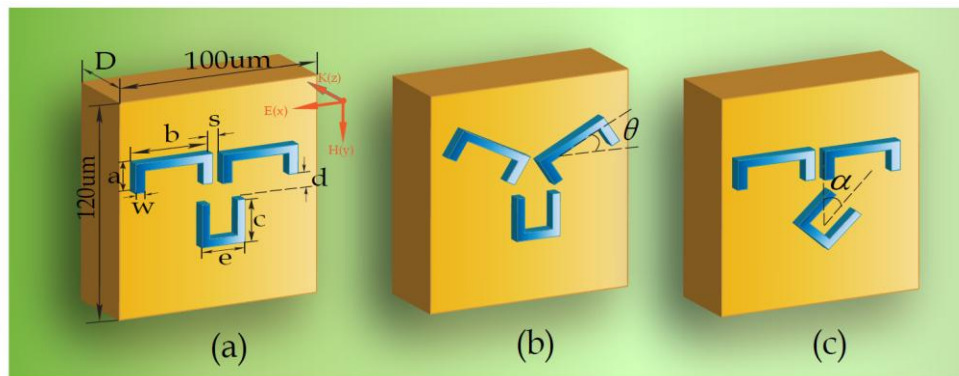


Fig. 1. Schematics of the TUR unit cells. (a) Geometric parameters of the TUR unit cell are $a = 19 \mu\text{m}$, $b = 42 \mu\text{m}$, $c = 28 \mu\text{m}$, $e = 29 \mu\text{m}$, $s = 3 \mu\text{m}$, $w = 5 \mu\text{m}$, and $d = 12 \mu\text{m}$. The thickness of the aluminum microstructure is 200 nm . The periods are $100 \mu\text{m}$ in the x direction and $120 \mu\text{m}$ in the y direction. The external electric field is along the x direction; (b) twisting the DURs; (c) rotating the SUR.

response of the metamaterial structure gets significantly modified and can even disappear owing to the violation of the design requisite.

2. Measured results and numerical analysis

The PIT “metamaterial molecule” consists of three-U-shape resonators (TUR) in a unit cell, as shown in Fig. 1(a). To satisfy the requirements for the PIT design rule described above, the lower single-U resonator (SUR) is designed with long arms and a short base and serves as the high- Q mode with a narrow spectral linewidth, while the upper double-U resonator (DUR) has short arms and long bases, generating a broad spectral linewidth (as the low- Q mode) because

of a larger dipolar moment and hence a stronger coupling with the free space radiation. The Q factor of the resonators is manipulated in our design by gradually rotating the U-shape elements, as shown in Figs. 1(b)-1(c).

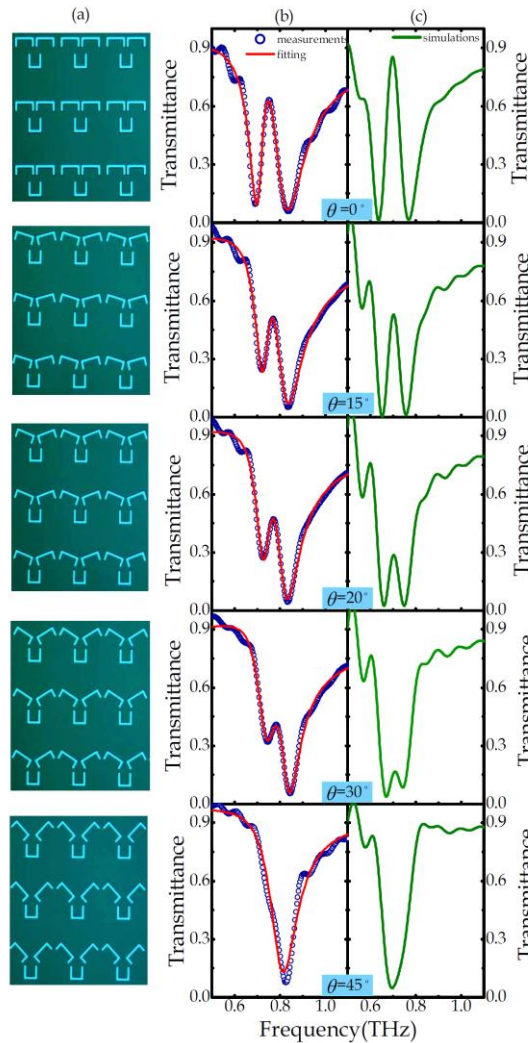


Fig. 2. (a) Optical images of the TURs with twisted DURs of various angles θ . (b) The blue circles and the pink solid lines represent the measured and the fitted transmission spectra, respectively, for different twisting angles θ . (c) Simulated transmission spectra (green solid lines) for different twisting angles θ .

The rectangular sample array of 200-nm-thick aluminum film was fabricated on a 640- μm -thick n-type silicon substrate by conventional optical lithography. Resonant properties of all samples were measured by use of an 8- f , broadband (0.1-4.5 THz) confocal terahertz time domain spectroscopy system under normal incidence and with electric field parallel to the gap of the U-shape resonators [27–31]. The absolute amplitude transmittance is defined as $|\tilde{T}(\omega)| = |\tilde{E}_s(\omega)/\tilde{E}_r(\omega)|^2$, where $\tilde{E}_s(\omega)$ and $\tilde{E}_r(\omega)$ are Fourier transformed frequency-dependent amplitudes of the terahertz pulse transmitted through the array and the reference blank silicon wafer, respectively.

In the first step, we rotate the orientation of both elements in the DUR in opposite directions with various angles $\theta = 0^\circ, 15^\circ, 20^\circ, 30^\circ$ and 45° . As illustrated in Figs. 2(a) and 2(b), in the absence of twisting, i.e. $\theta = 0^\circ$, a fully resolved PIT spectral response is observed with a transparency window located at 0.75 THz and has a 63% transmittance between two resonance dips at 0.69 THz and 0.84 THz [26]. As we gradually rotate each of the double U-shape resonators, modulation of the PIT spectral response is observed. The transmission peak intensity is declined with gradual disappearance of the lower frequency resonance dip at 0.69 THz and eventually when $\theta = 45^\circ$, the spectrum degenerates to a single resonance transmission dip at 0.83 THz and the PIT response disappears.

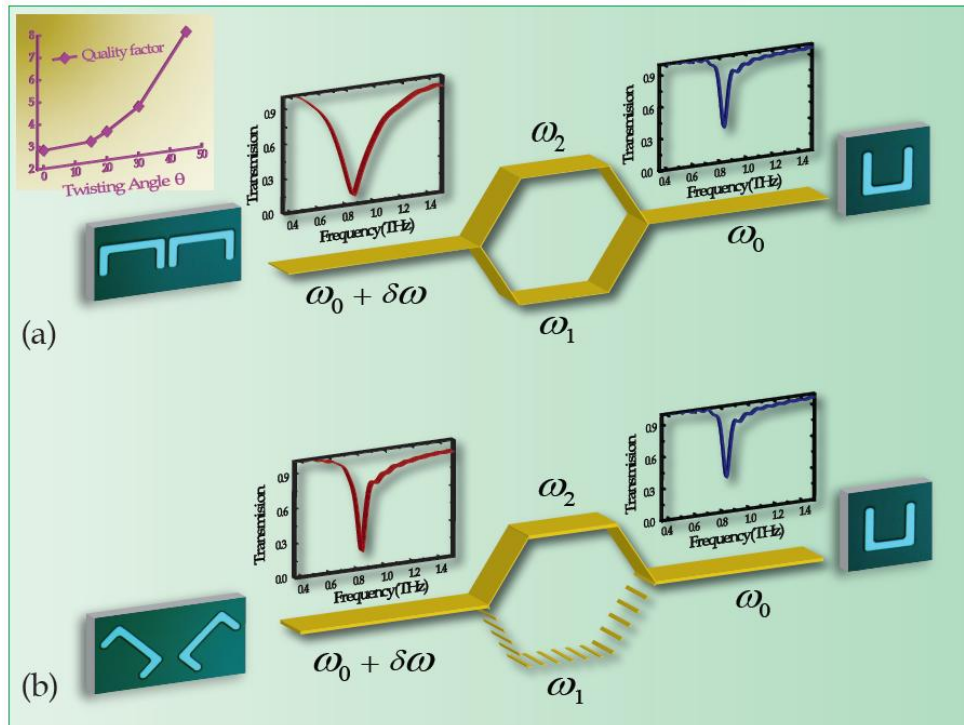


Fig. 3. (a) Existence of splitting two energy levels when two resonances have same frequency but significantly contrasting linewidths. (b) Absence of splitting two energy levels when two resonances are located at the same frequency and with comparable linewidths.

The underlying mechanism of the PIT modulation can be understood as follows. Without twisting, the resonances of SUR and DUR are almost perfectly aligned with a negligible frequency detuning of less than 0.015 THz and with distinct Q factors of 12.41 and 2.82 (the Q factor was obtained from the resulting transmission curves, $Q = \omega_0 / \Delta\omega$, where ω_0 is the resonance frequency and $\Delta\omega$ is the full width at half maximum bandwidth). As a result, the coupling through near-field interaction leads to splitting into two new discrete energy levels, as depicted in Fig. 3(a). The transmission peak at 0.75 THz arises from the splitting of the two new resonances (plasmonic modes), i.e. a lower-frequency mode $|\omega_1\rangle$ at 0.69 THz and the higher-frequency mode $|\omega_2\rangle$ at 0.84 THz [32]. Note that when changing the twist angle of DUR from $\theta = 0^\circ$ to $\theta = 45^\circ$, the Q factor of the DUR resonance gradually increases from 2.82 to 7.25 as a result of the reduced coupling with the external exciting field and the destructing of its inward-radiant mechanism, as shown in the inset of Fig. 3(a), which leads to comparable Q factors between the SUR and the twisted-DUR modes. According to the design guideline of PIT, no remarkable PIT effects would occur under such circumstance, which is

also consistent with our observation. We consider that the increase of θ not only causes an increase in the Q factor of the DUR resonance, but also leads to decrease in coupling between two plasmonic resonance modes. As a result, it would not lead to splitting into two new discrete resonances, as described in Fig. 3(b). The absence of energy level splitting contributes to the degeneration of transparent window in the transmission spectrum.

Under certain conditions, i.e. (i) sufficiently small frequency detuning between the two coupled resonances; (ii) strongly contrasting resonance linewidths; and (iii) appropriate resonance amplitudes, PIT effect can be regarded as an analogue of Fano-type resonances [33–35]. We noticed that the aforementioned conditions in Fano-type resonances are also quite consistent with the design rule of the PIT effect. We calculated the transmittance using a Fano-type model [33,36]:

$$T \propto \sum_i \frac{(\varepsilon_i + q_i)^2}{1 + \varepsilon_i^2}, \left(\varepsilon_i = \frac{\omega - \omega_i}{\gamma_i/2}, \text{ in our case } i = 1, 2 \right) \quad (1)$$

Here, the frequency ω_1 (ω_2), linewidth γ_1 (γ_2) and the Breit-Wigner-Fano coupling coefficient q_1 (q_2) characterize the feature of the left-side (right-side) dip. With parameters shown in Table 1, the calculated transmittances based on Eq. (1) reproduce all the experimental results quite well, as shown by the solid curves of Fig. 2(b). It is found that the linewidth of the left-side dip γ_1 increases from 0.075 to 0.104 THz when altering θ from 0° to 30° , and for the case of $\theta = 45^\circ$, specifically, this linewidth increases to a large numerical value, which leads to the degeneration of the lower energy resonance as well as the splitting of two new resonance dips.

Table 1. Parameters used in the Fano Model to fit the transmittance with twisted DURs

θ	$\omega_1/2\pi$ (THz)	$\omega_2/2\pi$ (THz)	$\gamma_1/2\pi$ (THz)	$\gamma_2/2\pi$ (THz)	q_1	q_2
0°	0.706	0.801	0.075	0.156	0.2947	-0.4263
15°	0.727	0.808	0.079	0.132	0.1509	-0.4909
20°	0.728	0.811	0.082	0.115	0.0478	-0.4632
30°	0.735	0.828	0.104	0.096	-0.1638	-0.4100
45°	-	0.804	-	0.143	-	-0.1628

The measured characteristic spectral responses of the TUR structures are further supported by a full wave numerical simulation using CST Microwave Studio, as shown in Fig. 2(c). The unit cell shown in Fig. 1 was used in the simulation with periodic boundary conditions. The substrate silicon was modeled as a lossless dielectric $\varepsilon = 11.78$ and Al was simulated with a default conductivity of $\sigma = 3.72 \times 10^7 \text{ S}\cdot\text{m}^{-1}$. Our numerical simulation reveals good agreement with the experimental results, as shown in Fig. 2(c). Figures 4(a)-4(f) depict the simulated surface current density and electric field distributions. From $\theta = 0^\circ$ to 45° , we observe a gradual transfer of electromagnetic energy from the SUR to DUR in surface current density and electric field distributions. When no twist is involved, the resonant excitation of the DUR mode is suppressed due to the destructive coupling between the DUR and SUR and most of the energy is concentrated in the SUR, as shown in Figs. 4(a) and 4(d). By increasing the twist angle θ , there is gradual transfer of energy from the SUR to DUR. Consequently, at $\theta = 45^\circ$, the DUR becomes highly radiative whereas the resonance of SUR, which acts as a subradiant resonator, completely disappears, leading to the degeneration of PIT spectral response, as shown in Figs. 4(c) and 4(f) [37,38]. By rotating the DUR, its two inner arms are segregated from each other, therefore destructing the inward-radiant mechanism which is

critical to the low Q of the DUR resonance and further violating the scheme of two resonant modes with significant difference in Q factors, as shown in Fig. 3(b).

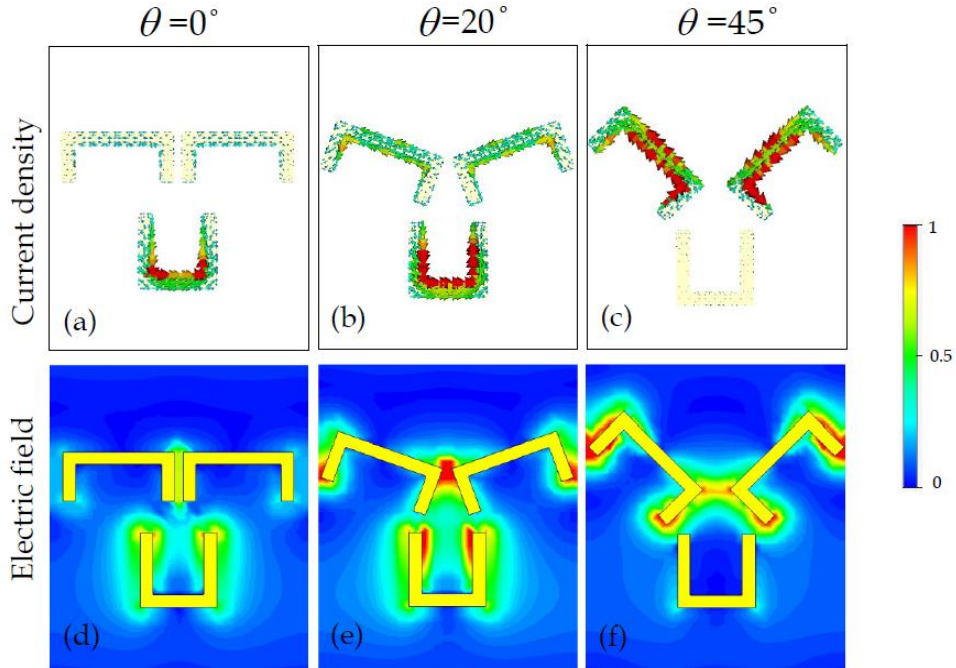


Fig. 4. Current density (a)-(c) and electric field distributions (d)-(f) of the TUR structures for different twisting angles θ of the DUR.

To further understand the characteristics of the Q -factor-induced PIT modulation, we investigate another variation by rotating the SUR instead of the DUR, with $\alpha = 0^\circ, 30^\circ, 70^\circ, 90^\circ$, as shown in Figs. 1(c) and 5(a). Similar phenomena of the PIT modulation can be observed with the transmission peak at 0.75 THz going down from 63% to 44% and the higher energy resonance dip at 0.84 THz gradually vanishes, leading to the degeneration of the PIT window, as illustrated in Figs. 5(b) and 5(c). Corresponding Fano fitting to the experimental spectra is shown in Fig. 5(b) and relative parameters are presented in Table 2.

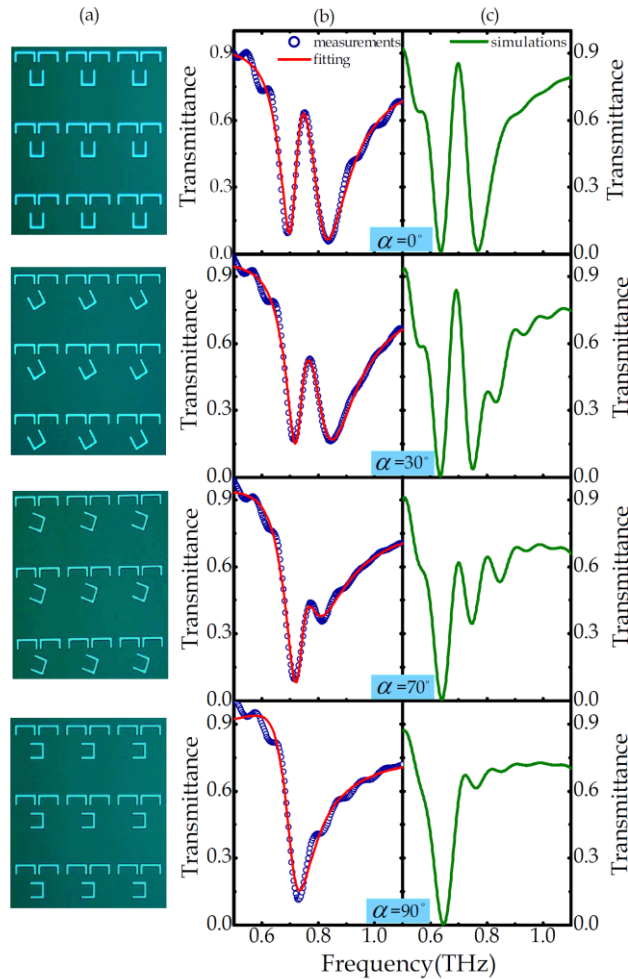


Fig. 5. (a) Optical images of the TURs with twisted SURs of various angles α . (b) The blue circles and the pink solid lines represent the measured and the fitted transmission spectra, respectively, for different twisting angles α . (c) Simulated transmission spectra (green solid lines) for different twisting angles α .

Table 2. Parameters used in the Fano Model to fit the transmittance with twisted SURs

α	$\omega_1/2\pi$ (THz)	$\omega_2/2\pi$ (THz)	$\gamma_1/2\pi$ (THz)	$\gamma_2/2\pi$ (THz)	q_1	q_2
0°	0.706	0.801	0.075	0.156	0.2947	-0.4263
30°	0.726	0.807	0.077	0.185	0.2926	-0.4643
70°	0.734	0.750	0.084	0.165	0.6307	-0.6595
90°	0.707	-	0.118	-	-0.4515	-

Figures 6(a)-6(f) depict the simulated surface current density and electric field distributions in ranging α from 0° to 90°. By rotating the SUR from 0° to 90°, we note that the orientation of the gap of SUR becomes non-parallel to the electric field of the incident beam. The excitation strength of the twisted SUR by external field, which is the projection of the electric field on the direction of the twisted angle, reduces significantly, leading to the

decreased resonant transmission amplitude of SUR and the excitation of SUR is completely quenched when $\alpha = 90^\circ$, thus leading to the degeneration of the PIT spectral response.

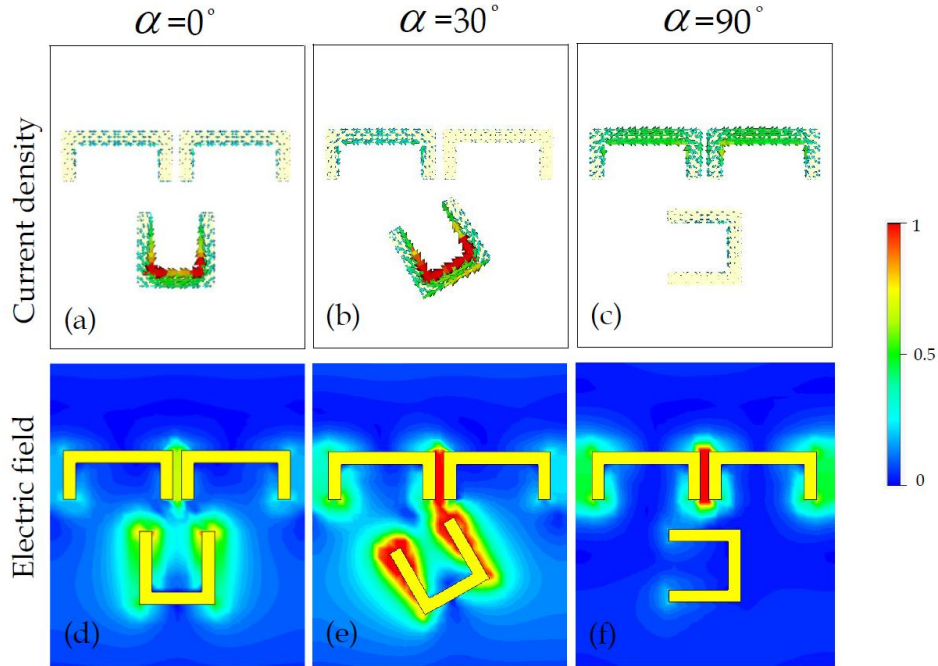


Fig. 6. Current density (a)-(c) and electric field distributions (d)-(f) of the TUR structures for different twisting angles α of the SUR.

3. Conclusion

In conclusion, we study the role of mutual twist in coupled resonators, giving rise to tunable PIT effect. It is demonstrated numerically and experimentally that the PIT effect can be manipulated by rotating either the subradiant or the superradiant resonators. The modulation of transparency peak is caused by shrinking the Q factor contrast between two modes. Their behavior with varying degree of twist is very well predicted by the Fano model and further corroborated by looking at the corresponding surface currents and electric field distributions. This work demonstrates that in order to maintain a sharp transparency peak, the coupled resonators must have contrasting Q factors. Otherwise the PIT effect tends to degenerate and the transparency peak disappears. The design discussed here would open up avenues for the development of tunable slow light devices not only in the terahertz domain but also across the entire electromagnetic spectrum.

Acknowledgments

This work was supported by the National Science Foundation of China (Grant Nos. 61028011, 61007034, and 60977064), the U.S. National Science Foundation, the Tianjin Sci-Tech Program (Grant Nos. 09ZCKFGX01500 and 10JCYBJC01400), and the MOE 111 Program of China (Grant No. B07014).